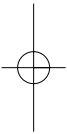
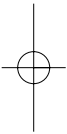


## 23

# Biofilm monitoring by photoacoustic spectroscopy

---

*T. Schmid, U. Panne, C. Haisch and R. Niessner*

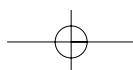


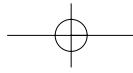
### 23.1 INTRODUCTION

Biofilms are layers of microorganisms and biopolymers (extracellular polymer substances, EPSs), which occur at the interfaces of aqueous systems. The unwanted growth of biofilms in process waters is termed biofouling and is responsible for a decrease in water quality and an increase of the frictional resistance in tubes. Despite these negative effects, biofilms are used as well in beneficial applications, e.g. removal of organic and inorganic pollutants in wastewater treatment plants (Wilderer and Characklis, 1989). For improvement of anti-fouling strategies and process optimization in wastewater treatment plants, a non-destructive method for on-line monitoring of biofilms is needed. A new photoacoustic technique allows non-destructive *in situ* monitoring of growth, detachment and thickness of biofilms. Main components of the biofilm can be determined by wavelength-dependent measurements in a depth-resolved fashion.

### 23.2 PHOTOACOUSTIC SPECTROSCOPY

Photoacoustic spectroscopy is based on the absorption of electromagnetic radiation inside a sample, where non-radiative relaxation processes convert the absorbed





#### 444 Control of biofilms

energy into heat. Due to the thermal expansion of the medium, a pressure wave is generated, which can be detected by microphones or piezoelectric transducers (Rosenzweig, 1980). The amplitude  $p$  of a photoacoustic signal generated by a laser pulse inside solid or liquid samples can be generally described by

$$p \propto \frac{\beta c^2}{C_p} E_0 \mu_a, \quad (23.1)$$

where  $C_p$  is the heat capacity,  $\beta$ , the thermal expansion coefficient,  $c$ , the speed of sound in the medium under study,  $E_0$ , the laser-pulse energy, and  $\mu_a$ , the optical absorption coefficient of the sample (Tam, 1986). After normalization of the signal with regard to laser-pulse energy and temperature, the absorption coefficient of the sample can be determined, which depends linearly on the concentration of the absorbing compound.

If short laser pulses are used for excitation, a time-resolved recording of the photoacoustic signal allows a depth-resolved investigation of the light absorption inside the irradiated part of the sample (Karabutov *et al.*, 1995). The distance between an absorbing object inside the sample and the sample surface can be calculated as

$$z = c \cdot t \quad (23.2)$$

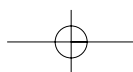
where  $t$  is the time delay between the laser pulse and the arrival of the pressure wave at the sample surface. Thus, changes in the optical absorption properties of a sample can be investigated depth resolved, if the sound velocity inside the sample is known.

### 23.3 PHOTOACOUSTIC BIOFILM MONITORING

#### 23.3.1 Experimental setup

Photoacoustic sensor heads for biofilm monitoring consist of a piezoelectric detector, which is coupled to a transparent prism (Figure 23.1). The biofilm grows directly on the surface of the prism and is illuminated by short laser pulses. The electromagnetic radiation is absorbed inside the biofilm, where a pressure wave is generated by the photoacoustic effect. The laser-induced pressure waves are detected by the piezoelectric transducer consisting of a 25  $\mu\text{m}$  thick poly(vinylidene fluoride) (PVDF) film. The transducer has a diameter of 5 mm allowing a representative area of 20  $\text{mm}^2$ . The detection limit for the optical absorption coefficient is 0.02  $\text{cm}^{-1}$  (Schmid *et al.*, 2002a) and the depth resolution in aqueous samples (e.g. aqueous solutions, hydrogels, biological matrices) is approximately 10  $\mu\text{m}$  (Kopp and Niessner, 1999).

The laser pulses are guided via optical fibers (550  $\mu\text{m}$  diameter, HCG-MO550T-10, Laser Components, Santa Rosa, USA) from the laser to the sensor head. In this study, a frequency-doubled Nd:YAG laser ( $\lambda = 532 \text{ nm}$ , Surelite 10-I,



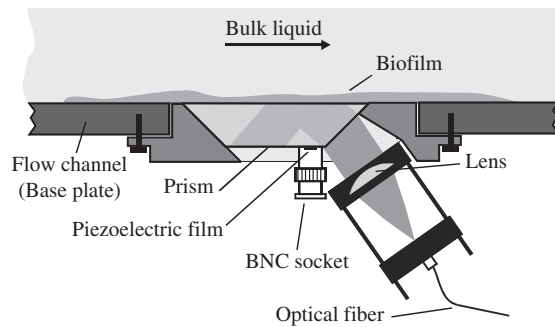


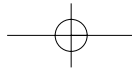
Figure 23.1 Photoacoustic sensor head for biofilm monitoring.

Continuum, Santa Clara, USA) and a tunable optical parametric oscillator (OPO, Panther, Continuum, Santa Clara, USA) were used for excitation of photoacoustic signals. The OPO allows the generation of laser pulses with wavelengths from 410 nm in the visible (Vis) to 2550 nm in the near-infrared range (NIR). The pre-amplified photoacoustic signal is recorded by a digital storage oscilloscope (TDS 540, Tektronix, Beaverton, USA). The synchronization of the oscilloscope with the laser pulse is performed with a trigger signal. All components of the sensor system are controlled by an in-house developed LabVIEW software (LABView 5.1, National Instruments, Austin, USA): flash lamp and shutter of the laser via a serial interface and the digital storage oscilloscope via the IEEE 488 bus.

For extensive characterization of the new biofilm monitoring technique, an 18-l tube reactor for growth of microorganisms was set up. The reactor contained a mixture of microorganisms taken from an aerobic sequencing batch biofilm reactor and fed by a nutrient solution consisting of  $690 \text{ mg l}^{-1}$  sodium acetate,  $60 \text{ mg l}^{-1}$  potassium dihydrogenphosphate,  $252 \text{ mg l}^{-1}$  ammonium sulfate,  $19 \text{ mg l}^{-1}$  potassium chloride and  $4 \text{ mg l}^{-1}$  yeast extract. The reactor was aerated with compressed air with a volume flow of  $1 \text{ l min}^{-1}$ . To generate biofilms on solid surfaces, the content of the tube reactor was pumped through a flow channel (100 ml volume; 260 mm long) by a peristaltic pump. For investigation of biofilms at different positions, three photoacoustic sensor heads were integrated into the base plate of the channel. A more detailed description of the experimental setup can be found in Schmid *et al.* (2002a).

### 23.3.2 Photoacoustic signals of biofilms

Figure 23.2 shows a typical photoacoustic signal profile of a biofilm measured at a wavelength of 532 nm. According to Equation (23.2), the time scale of the oscilloscope was converted into the corresponding depth scale. The conversion factor was the speed of sound inside the biofilm system. Water is the predominant component of both the biofilm and the bulk liquid phase. Therefore, the sound



## 446 Control of biofilms

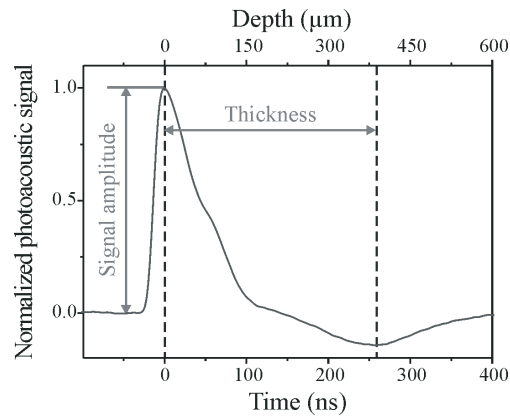


Figure 23.2 Typical photoacoustic signal profile of a biofilm ( $\lambda = 532 \text{ nm}$ ).

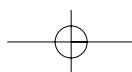
velocity of water, i.e.  $c = 1.5 \times 10^3 \text{ m s}^{-1}$  can be assumed for the biofilm system. The origin of the abscissa at  $0 \text{ } \mu\text{m}$  corresponds to the surface of the prism.

As exhibited in Equation (23.1), the amplitude of the photoacoustic signal is a function of the optical absorption coefficient, which depends linearly on the concentration of the absorbing compound. Most of the photoacoustic biofilm measurements presented in this chapter were performed at  $532 \text{ nm}$ . In the Vis spectral range, the incident light is absorbed by various pigments inside the cells and the EPS matrix. Therefore, the photoacoustic signal amplitude depends on the density of the immobilized biomass.

In most cases, the maximum of the signal corresponding to the highest biofilm density is at  $0 \text{ } \mu\text{m}$  and, therefore, directly on the surface of the sensor head. For the whole depth range inside the absorbing and scattering biofilm, the signal has a positive value. At the interface between biofilm and water, the signal becomes negative and reaches its minimum. Thus, the biofilm thickness can be determined by measuring the distance between the maximum and minimum of the photoacoustic signal profile.

This possibility for biofilm thickness measurements was discovered by measurements of biofilm models. The biofilm models consisted of agar–agar hydrogel layers with well-defined thickness containing enclosed iron(III) oxide particles. To simulate an aqueous bulk phase, water was added to the surface of the layers. In this way, the acoustic properties of biofilms could be modeled by agar–agar and the optical properties by iron(III) oxide particles, which absorb and scatter laser radiation at  $532 \text{ nm}$ .

The thickness measurements were validated by confocal laser-scanning microscopy (CLSM) using real biofilms grown on glass slides. The result of the photoacoustic thickness measurement was in good agreement with the independent microscopic-imaging technique (Schmid *et al.*, 2002a).



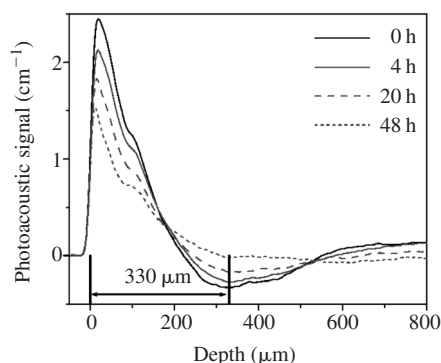


Figure 23.3 Biofilm detachment caused by a pH shift from 8.4 to 11.1. Depth-resolved photoacoustic measurements at 532 nm.

### 23.3.3 Photoacoustic biofilm measurements

In order to examine the new photoacoustic biofilm monitoring technique, biofilms were generated on the surfaces of the three sensor heads inside the flow channel. Subsequently, one of the process parameters (e.g. flow conditions, pH) was changed and modifications in biofilm density and thickness were monitored on-line by photoacoustic measurements.

Biofilm growth could be monitored by plotting the photoacoustic signal amplitudes versus time. The increase in signal intensity reflects the attachment of microbial cells and EPS molecules to the sensor surfaces and the corresponding increase of the density of the immobilized biomass (Schmid *et al.*, 2001). Due to different flow conditions at the three positions inside the flow channel, biofilms with different density and, in particular, different structure were formed on the sensor surfaces. The influence of flow conditions on the biofilm structure could be verified by generation of biofilms at different flow velocities. The experiments revealed that an increase in flow velocity leads to a shift of the biomass towards the solid surface and, therefore, to the formation of thinner biofilms (Schmid *et al.*, 2002a).

Biofilm detachment caused by dissolved as well as colloidal substances was monitored by depth-resolved measurements. The pH influences electrostatic interactions between EPS molecules and has, therefore, an indirect influence on the stability of the biofilm. After a pH shift from 8.4 to 11.1, biofilm detachment could be observed over several hours (Figure 23.3). The minimum of the photoacoustic signal at 330  $\mu\text{m}$  reflects the interface region between biofilm and bulk liquid. The measured biofilm thickness was approximately constant during the detachment process. It could be concluded that biofilm aggregates, which are smaller than the representative area of the sensor (20  $\text{mm}^2$ ) were detached from the biofilm surface. Thus, biofilm detachment caused by pH shifts can be interpreted as erosion of microscopic aggregates (Schmid *et al.*, 2002a, b)

The photoacoustic monitoring technique was used for an extensive investigation of various anti-fouling strategies. The effect of hydrogen peroxide on biofilms

## 448 Control of biofilms

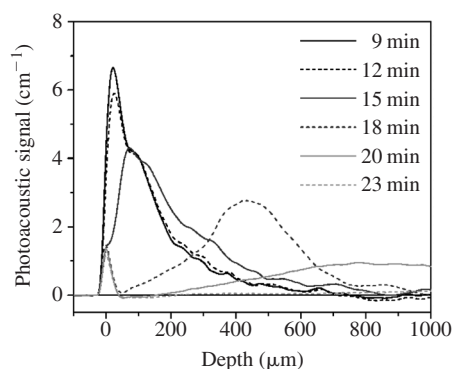


Figure 23.4 Biofilm detachment by 200 ppm hydrogen peroxide ( $\lambda = 532$  nm).

was compared with diverse isothiazolinone biocides. Biofilm removal by the oxidant hydrogen peroxide was the most effective anti-fouling strategy in this context. Most of the adsorbed biomass was removed within a few minutes. The changes in signal shape and biofilm thickness indicate that sloughing off of relatively large areas of the biofilm lead to the fast biofilm detachment (Figure 23.4).

Even the interaction of biofilms with particulate matter can be investigated by photoacoustic measurements. The sorption of iron(III) oxide particles ( $<5 \mu\text{m}$ ) could be observed on-line. Sorbed particles can influence the stability of the biofilm and, therefore, lead to a partial detachment. This was observed by depth-resolved measurements. Predominantly, the part of the biofilm with the highest particle concentration was removed from the sensor surface. The particles could not reach the base biofilm. Therefore, detachment effects in this part of the film were relatively weak (Schmid *et al.*, 2002a).

By use of a tunable OPO, photoacoustic absorption spectra of biofilms were determined. Absorption bands of main components, such as pigments, water and carbohydrates could be identified in the Vis and NIR spectra. Depth-resolved measurements revealed the possibility to investigate the distribution of chemical compounds inside the biofilm system (Schmid *et al.*, 2002c).

## 23.4 CONCLUSIONS

Photoacoustic spectroscopy is an interesting approach to biofilm monitoring. The new technique allows *in situ* monitoring of growth, detachment and thickness of biofilms. Detachment mechanisms can be elucidated by depth-resolved measurements. By photoacoustic spectroscopy, the influence of various physical and chemical factors, such as flow conditions or pH-value was investigated. Additionally, diverse anti-fouling strategies could be compared to each other.

Wavelength-dependent measurements allow the depth-resolved determination of main components of the biofilm system due to their characteristic

## Biofilm monitoring by photoacoustic spectroscopy 449

absorptions. Within further studies, specific staining reagents will be used to distinguish, e.g. between living and dead cells. Stained cells and EPS components will be detected by photoacoustic measurements at specific wavelengths in a depth-resolved fashion.

### *Acknowledgements*

The authors acknowledge the financial support by Deutsche Forschungsgemeinschaft (DFG) and a grant awarded to Thomas Schmid by Max-Buchner-Forschungsförderung (MBFSt).

### REFERENCES

- Karabutov, A.A., Podymova, N.B. and Letokhov, V.S. (1995) Time-resolved photoacoustic detection of absorbing particles in scattering media. *J. Mod. Opt.* **42**, 7–11.
- Kopp, C. and Niessner, R. (1999) Depth-resolved determination of the absorption coefficient by photoacoustic spectroscopy within a hydrogel. *Anal. Chem.* **71**, 4663–4668.
- Rosencwaig, A. (1980) *Photoacoustics and Photoacoustic Spectroscopy*, Wiley, New York.
- Schmid, T., Kazarian, L., Panne, U. and Niessner, R. (2001) Depth-resolved analysis of biofilms by photoacoustic spectroscopy. *Anal. Sci.* **17**, 574–577.
- Schmid, T., Panne, U., Haisch, C., Hausner, M. and Niessner, R. (2002a) A photoacoustic technique for *in situ* monitoring of biofilms. *Environ. Sci. Technol.* **36**, 4135–4141.
- Schmid, T., Panne, U., Haisch, C. and Niessner, R. (2002b) Biofilm monitoring by photoacoustic spectroscopy (PAS). *Water Sci. Technol.*, in press.
- Schmid, T., Panne, U., Haisch, C. and Niessner, R. (2002c) Photoacoustic absorption spectra of biofilms. *Rev. Sci. Instrum.*, in press.
- Tam, A.C. (1986) Applications of photoacoustic sensing techniques. *Rev. Mod. Phys.* **58**, 381–431.
- Wilderer, P.A. and Characklis, W.G. (1989) *Structure and Function of Biofilms*, Wiley-Interscience, New York.